Published in final edited form as:
Nat Mater. 2015 October ; 14(10): 996–1001. doi:10.1038/nmat4368.

Eliminating degradation and uncovering ion-trapping dynamics in electrochromic WO_3 thin films

Rui-Tao Wen, **Claes G. Granqvist**, and **Gunnar A. Niklasson**
Department of Engineering Sciences, The Ångström Laboratory, Uppsala University, P. O. Box 534, SE-75121 Uppsala, Sweden

Abstract

Amorphous WO_3 thin films are of keen interest as cathodic electrodes in transmittance-modulating electrochromic devices. However, these films suffer from ion-trapping-induced degradation of optical modulation and reversibility upon extended Li^+-ion exchange. Here, we demonstrate that ion-trapping-induced degradation, which is commonly believed to be irreversible, can be successfully eliminated by constant-current-driven de-trapping, *i.e.*, WO_3 films can be rejuvenated and regain their initial highly reversible electrochromic performance. Pronounced ion-trapping occurs when x exceeds ~0.65 in Li_xWO_3 during ion insertion. We find two main kinds of Li^+-ion trapping sites (*intermediate* and *deep*) in WO_3, where the *intermediate* ones are most prevalent. Li^+-ions can be completely removed from *intermediate* traps but are irreversibly bound in *deep* traps. Our results provide a general framework for developing and designing superior electrochromic materials and devices.

Keywords

WO_3 films; electrochromic; variable-transmittance windows; ion-trapping

Electrochromism is an enabling technology for variable-transmittance windows in energy-efficient architecture, non-emissive information displays, variable-reflectance mirrors, and other applications[1,2]. The most well-developed electrochromic technology is based on intercalation/deintercalation of small ions in electrode materials. Amorphous WO_3 is the best known electrochromic material and is used in today's "smart" windows[2-4]. Thin films of WO_3 can color from a transparent state to deep blue by Li^+-ion insertion under a low voltage bias, and the films return to their transparent state by Li^+-ion extraction if the voltage bias is increased. The operational voltage range is typically 2.0–4.0 V *vs.* Li/Li^+. It is widely accepted that the intercalation/deintercalation process, in the case of a Li^+-conducting electrolyte, can be written as[5]

Correspondence should be addressed to: Ruitao.Wen@angstrom.uu.se.
Author contributions: R-T. W conceived the idea, designed and performed the experiments. R-T. W carried out the data analysis with help from G.A.N and C.G.G. R-T. W, G.A.N and C.G.G. co-wrote the manscript. G.A.N and C.G.G. supervised and supported the work.

Europe PMC Funders Author Manuscripts

$$\mathrm{WO_3} + x\left(\mathrm{Li^+} + e^-\right) \leftrightarrow \mathrm{Li}_x\mathrm{WO_3} \quad , \qquad (1)$$

where x is the mole fraction of lithium inserted into a WO_3 host and e^- denotes electrons. Coloration is an electronic process, and optical absorption is attributed to intervalence electron transfer from W^{5+} to W^{6+} sites[6].

Large optical modulation and long-term durability are key prerequisites for practical implementation of electrochromic devices. However, degradation of their optical modulation is typically observed after several hundreds or thousands of cycles, and lifetime is also crucially dependent on the operational voltage range[5,7,8]. Specifically, it has been shown that all Li^+-ions inserted during coloration cannot be extracted[7,9] and, over many cycles, these bound ions accumulate in the film and erode the electrochromic effect. The irreversibility becomes more pronounced as the lower potential limit is decreased below 2 V *vs.* Li/Li^+, (**ref.**10). The physical and chemical bases of the irreversibility remain poorly known, experimentally as well as theoretically. Moreover, a number of Li-based compounds may form at low potentials at interfaces or in the host material[11-13].

It has been argued that Li^+ ions become localized close to W^{5+} color centers, probably by binding to oxygen coordination shells of W^{5+} sites[14]. The kinetics of electrochromic coloration is very similar to that of low-frequency ionic relaxation[15], which in its turn has been interpreted as being due to ion trapping[16], and hence it is likely that ion trapping/de-trapping is the rate-determining step for electrochromic coloration/bleaching. Theories of ion diffusion and relaxation have considered the possibility of co-existing traps of various types[14,17], or even a continuous distribution of trap energies in a multiple-trapping scenario[18,19]. Specifically, Bisquert[14,17] proposed that the host structure contains two types of sites: (*i*) a network of connected “shallow” sites (with low-energy barriers) allowing reversible and fast diffusion of ions throughout the film, and (*ii*) isolated “deep” sites surrounded by high-energy barriers where ions become immobile once trapped. The latter trapping sites can be filled by Li^+-ions with high energy or by waiting for a sufficiently long time.

Three questions now arise: *First*, given that degradation of electrochromism is due to ion trapping there must be a distribution of trap energies, and the specific question is whether the deeper-trapped Li^+-ions can be de-trapped by providing sufficiently high energy or by waiting for long-enough time? *Second*, does the film maintain its reversible electrochromism after de-trapping of these Li^+-ions? *Third*, does significant ion-trapping occur regardless of the value of x in Eq. (1), or will trapping take place only when x exceeds some “critical” value? This Letter addresses these questions on the basis of direct experimental observations of Li^+-ion trapping and de-trapping in WO_3 films; it demonstrates how electrochromic degradation can be eliminated and also elucidates details of the ion-trapping dynamics.

As described in detail in the Methods section, our WO_3 thin films were sputter-deposited onto glass pre-coated with transparent and electrically conducting layers. The films were amorphous, as confirmed by x-ray diffraction. Cyclic voltammetry (CV) in different

potential windows was used to insert/extract various amounts of charge. Voltage sweep rates in the 0.1–100 mV s^{-1} interval were employed in order to achieve slow to fast charge exchange. A galvanostatic technique, using a constant "loading current", was adopted to extract ions from trap sites. Optical transmittance was monitored by *in situ* measurements. The electrolyte was 1M $LiClO_4$ dissolved in propylene carbonate, and counter and reference electrodes were Li foils. All voltages refer to a Li/Li^+ reference.

Our first experiments employed a commonly used potential window for WO_3, *viz.*, 2.0–4.0 V. Severe reduction of CV scans and optical modulation can be observed after 400 cycles (Fig. 1a and 1c). These effects are assigned to ion-trapping-induced degradation; specifically the trapped ions yield charge accumulation in the film upon CV cycling so that the capacity for further charge insertion becomes lost. Correspondingly, the open circuit potential (OCP) decreases from an initial value of ~3.2 V to ~2.8 V after 400 CV cycles.

We conjectured it would be possible to extract the trapped Li^+-ions and rejuvenate the host material by applying a high-enough potential and, in order to test this idea, we performed a galvanostatic experiment and ran a constant loading current of ~1×10^{-5} A cm^{-2} through the WO_3 film for 20 h (Fig. 1b). The potential went from ~2.8 to ~5.5 V during this procedure whereas the optical transmittance remained almost unchanged (Fig. S1). When the film was kept for ~2 h after galvanostatic loading, the voltage dropped from ~5.5 V to a stable value of ~3.3 V without loss of optical transmittance (Fig. S1). This latter voltage is approximately the same as the OCP for the as-deposited state, which indicates that the trapped ions have successfully been de-trapped. Importantly, after de-trapping it is found (Fig. 1a, c and d) from CV data and optical measurements that the film has the same performance as in the initial state, thus confirming complete rejuvenation of the electrochromism. Analogous studies on WO_3 films with different levels of ion-trapping, induced by using a different number of CV cycles, verified that de-trapping could be accomplished and electrochromism regained. After de-trapping, the WO_3 films exhibit the same degradation features as before (Fig. S2) and the original CV data were recovered (Fig. 1a). We have also modified deposition conditions to obtain films with different degradation under CV cycling; these films could also be rejuvenated by our galvanostatic de-trapping procedure (Fig. S3).

However, when interpreting galvanostatic experiments it is important to consider electrochemical reactions in the electrolyte. Fig. 1b also shows a galvanostatic curve obtained by using an inert Pt electrode in the same electrolyte. This electrolyte response is indeed very similar to the response of the WO_3 electrode and it is clear that a large part of the applied current drives reactions in the electrolyte. There are only small differences between the curves in Fig. 1b**,** and it would be difficult to assign specific features to a de-trapping process in the film.

To shed more light on whether the constant loading current exerts the driving force to extract the trapped ions in WO_3, we performed galvanostatic measurements with a constant current of 1×10^{-5} A cm^{-2} for 20 h on films with a larger amount of trapped Li^+ ions than in the earlier experiments, and we also performed parallel measurements without applying any current but simply recording the OCP. Prior to applying the constant current, the WO_3 film

was cycled 20 times at 10 mV s^{-1} in a wider potential range than before, specifically at 1.5–4.0 V. Fig. 2a–d indicate that optical modulation now degrades rapidly already during the first few CV cycles. This degradation takes place both for the bleached and colored state, which is distinctly different from the data taken in the narrower voltage range of 2.0–4.0 V in which case only the colored state was affected (Fig. 1d). Furthermore, a minor but significant portion of the inserted ions could not be extracted from films cycled at 1.5–4.0 V, which is apparent from Fig. 2c that shows charge capacity, calculated by integrating the insertion/extraction parts of the CV data, during 20 cycles. After this number of cycles, OCP has shifted to ~2.2 V and optical modulation tends to a constant value. Our data (Fig. 2a and Fig. 2e) showed a significant difference between the galvanostatic de-trapping measurement and the parallel recording without applied current; the transmittance returned to its original magnitude—except for a slight difference at short wavelengths (Fig. 2d) which may be assigned to trapped ions—when the film was subjected to a constant current, whereas the transmittance was barely altered in the absence of any current (Fig. 2a) although the OCP increased slightly (by ~0.12 V). It is then evident that the trapped ions have to be extracted at a high potential, which can be attained by current loading. Degraded films for which no prior constant current was applied, could be forced to return to their original state by current loading at 1×10^{-5} A cm^{-2} for 20 h (Fig. 2e).

The galvanostatic curves for the degraded WO_3 film electrode showed qualitative differences from the electrolyte response obtained with the Pt electrode (Fig. 2e). In particular a plateau at ~5.1 V is seen only for the WO_3 electrode and clearly originates from processes in the film. We assign this feature to the ion de-trapping process. These results are very promising and clearly indicate that ion de-trapping can be distinguished from the underlying response of electrolyte reactions. Hence we conclude that ion-trapping-induced degradation of WO_3-based electrochromic films can be effectively avoided by the application of our galvanostatic de-trapping procedure.

The sweep rate for the CV scans is of obvious significance for the ion trapping/de-trapping dynamics and is considered next. Fig. 3a shows cyclic voltammograms for WO_3 films at 1.5–4.0 V for various scan rates, and Fig. S4 summarizes corresponding results for 1.7–4.0 and 2.0–4.0 V. The CV data were recorded by starting at 100 mV s^{-1} and gradually lowering the rate after each cycle until reaching 0.1 mV s^{-1}. Charge capacity is strongly dependent on scan rate (Fig. 3b), and greater Li^+-ion insertion takes place for increased potential window (Fig. 3c). When the scan rate is decreased in the potential windows 1.5–4.0 and 1.7–4.0 V, the total amount of inserted charge increases and reaches saturation at ~5 mV s^{-1} and ~2 mV s^{-1}, respectively, whereas the inserted charge still increases until 0.1 mV s^{-1} (~12 h for one cycle) at 2.0–4.0 V, thus indicating that the ultimate charge capacity has not been reached at the latter scan rate. There is a large difference between inserted and extracted charge capacity—*i.e.*, the amount of inserted Li^+-ions is greater than the one that can be extracted—beginning at a certain scan rate, implying that a fraction of inserted Li^+-ions remains in the WO_3 films. Ion-trapping sets in at ~40, 20 and 0.5 mV s^{-1} for the potential windows 1.5–4.0, 1.7–4.0 and 2.0–4.0 V, respectively. Significant ion-trapping occurs when x exceeds ~0.65 in Li_xWO_3 (Fig. 3b), which is in excellent agreement with results in a previous study which showed that Li^+-intercalation was reversible only when $x < 0.7$ for WO_3, **(ref.**20**)** and

well above a value of 0.3–0.35 that serves as a "rule-of-thumb" for safe long-term device operation[2]. Our present value of x is almost independent of scan rate and potential window, thus demonstrating that pronounced ion trapping above a certain *critical* density of Li^+-ions is a general feature for WO_3 films.

Ion-trapping becomes increasingly severe as the scan rate is lowered beyond the point where this phenomenon sets in. In the 1.5–4.0 V range, for example, the inserted charge reaches a peak at 5 mV s^{-1}. The inserted charge begins to drop at lower scan rates and it is evident that the extracted charge shows a concomitant decrease. One concludes that ion-trapping sites in WO_3 become fewer and fewer until they are fully occupied. Inserted and extracted charge become approximately the same at ~0.5 mV s^{-1} (Fig. 3b). A constant loading current was applied to de-trap the Li^+-ions responsible for the optical degradation with the aim of obtaining recuperated optical transmittance. It is seen that the optical transmittance in the bleached state returned to that of the as-deposited state, except for a slight difference at short wavelengths (Fig. 3d) which cannot be eliminated by current loading. Our data therefore confirm the existence of irreversible trapping sites in the host. It should also be emphasized that the transmittance in the colored state after the de-trapping procedure was always very close to the initial one.

The voltammetric scan rate determines the charge capacity (Fig. 3b), and a related dependence is expected for the optical performance. This surmise is of considerable practical interest for electrochromic devices, for which the optical modulation range normally should be maximized while the modulation time should be optimized with regard to the specific application. Fig. 4a shows optical modulation at 550 nm for diminishing scan rate in the 1.5–4.0 V range, followed by ion de-trapping at 1×10^{-5} A cm^{-2} for 20 h and zero current for another ~2 h. The optical modulation was enlarged when the scan rate was gradually decreased to 30 mV s^{-1}; then there was a monotonic drop of the modulation when the scan rate was decreased still further, which signals the onset of strong ion-trapping. The optical transmittance can be recovered by ion de-trapping and remains constant when the loading current is removed. Full-spectrum and monochromatic (550 nm) transmittance data for the ranges 1.7–4.0 and 2.0–4.0 V are presented and compared in Fig. S5 and Fig. S6, respectively. Optical modulation at 550 nm for different potential windows—summarized in Fig. 4b—shows a slight decrease at very low scan rate (0.1 mV s^{-1}) for 2.0–4.0 V, where the drop is solely due to transmittance degradation in the colored state (Fig. S5). Peaks in the optical modulation were also seen for larger potential windows, and the peak position was displaced from 10 to 30 mV s^{-1} as the potential window was enlarged from 1.7–4.0 to 1.5–4.0 V. In contrast with the case of 2.0–4.0 V, the drop of optical modulation in the former two potential windows ensues from degradation of both colored and bleached states (Fig. S5b and Fig. 4c, which are discussed further below). Ion-trapping at 2.0–4.0 V became noticeable only when the scan rate was lower than 0.5 mV s^{-1} (or x exceeded ~0.65 in Li_xWO_3), and it can be concluded that ions are not irreversibly trapped to any large extent if WO_3 films are cycled in this range. Furthermore the optical transmittance after de-trapping is almost the same as for the initial film (Fig. 1d). The latter results highlight the fact that 2.0–4.0 V serves as an excellent potential window for the operation of WO_3-based electrochromic devices.

As noted above, present-day models for ion exchange in WO_3[14-17] indicate that one may distinguish between two different types of traps: *shallow* ones that are reversible and easy to populate/depopulate, and *deep* ones that are difficult to access and wherein ions become permanently trapped. The results of the present study point at the existence also of *intermediate* trapping sites from which ions can be extracted by applying a high-enough potential. Ions trapped in deep sites—whose existence is confirmed by slight differences at short wavelengths in optical spectra—are found to be much fewer than ions in intermediate sites.

The physical nature of the various traps can be elucidated by taking a closer look at the spectral optical data for W oxide films cycled at various rates at 1.5–4.0 V (Fig. 4c), especially for colored films. The spectral response is rather flat at 10 mV s^{-1}, while the transmittance drops towards increasing wavelengths for higher rates and increases from a low to a high value upon increasing wavelengths at lower rates. These results can be reconciled with those in Fig. 3b as follows: The data for 10 mV s^{-1} correspond to conditions where ion trapping becomes prevalent; results for higher rates pertain to conditions for reversible ion exchange where the optical absorption is well known to be associated with W^{5+} states and polaron absorption, whereas lower rates lead to severe ion trapping. The large short-wavelength absorption in the latter case can be associated with W^{4+} states, as investigated in detail in earlier work[20]. Data for 2.0–4.0 V indicate W^{5+} states (Fig. S5a) and insignificant ion trapping (Fig. 3b), and data for 1.7–4.0 V (Figs. S5b and Fig. S6b) are qualitatively similar to the case of 1.5-4.0 V. The presence of W^{4+} is interesting, and the intercalation of two Li^+ ions close to a tungsten site, together with charge balancing electrons can, after structural rearrangements, lead to the formation of local aggregates of lithium oxide (Li_2O) and/or lithium peroxide (Li_2O_2). Density functional computations have shown that Li ions inserted into WO_3 have their lowest total energy when positioned centrally between the neighboring oxygen ions[21]. Hence they “share” their bonds with a number of oxygens, which is believed to lead to much weaker bonds than the ionic ones in Li_2O and Li_2O_2 aggregates. It should also be noted that Li tungstates have been observed[13] in degraded amorphous WO_3 films, and it has been argued[22] that these compounds are formed at voltages below 2 V *vs.* Li^+. De-trapping of ions by ultraviolet irradiation[23] also remains as a subject for future consideration.

In conclusion, we have answered the questions posed in the Introduction and demonstrated that WO_3 films, subjected to long-term voltammetric cycling, can regain their initial electrochromic performance by a galvanostatic treatment capable of removing intermediate traps. However, the relevance of this technique to practical devices remains to be demonstrated. Ion-trapping is a ubiquitous phenomenon, but the trapped ions will not reach deep sites upon voltammetric cycling in the most commonly used potential window for WO_3, *viz.*, ~2.0–4.0 V *vs.* Li^+. Significant ion-trapping takes place when x exceeds a critical value in Li_xWO_3 (~0.65 in our study). There is no doubt that enhanced electrochromic performance can be obtained as we reach better understanding of the underlying processes of ion-trapping and energy barriers in WO_3, and this knowledge may open avenues towards superior smart windows and hence widen the scope for future buildings that are both energy efficient and benign for human occupation.

Methods

Thin film deposition

Thin films of WO_3 were deposited by reactive *dc* magnetron sputtering in a coating system based on a Balzers UTT 400 unit. The substrates were glass plates with transparent and electrically conducting layers of In_2O_3:Sn (known as ITO) having a sheet resistance of 60 Ω. No substrate heating was used during the deposition. The sputter target was a 5-cm-diameter plate of metallic tungsten (99.95%). Prior to sample deposition, the chamber was evacuated to ~6×10^{-5} Pa. Pre-sputtering took place in argon (99.998%) for five minutes, and oxygen (99.998%) was then introduced. During deposition, the O_2/Ar gas-flow ratio was set at a constant value of 13%. The total pressure during sputtering was maintained at ~30 mTorr in the case of films, for which data are presented in this paper, and the power to the target was 200 W. The film thickness d was 270 ± 5 nm as determined by surface profilometry with a DektakXT instrument. This study is based on results from about ten WO_3 films. The chosen deposition parameters lead to porous films that were suitable for degradation studies. Similar films have been studied in other recent work of ours[8]. More compact films show better durability, but at the cost of slower coloration kinetics. We have also studied films with different durability, obtained by varying the pressure during sputtering in the range 20-40 mTorr (Fig. S3). As is generally the case for sputter deposited oxide films, a minor amount of water is expected to be incorporated during deposition.

Structural and compositional characterization

Film structures were determined by x-ray diffraction (XRD) using a Siemens D5000 diffractometer operating with CuK_α radiation at a wavelength of 0.154 nm. XRD analysis indicated amorphous structures. Elemental compositions and atomic concentrations were determined by Rutherford Backscattering Spectrometry (RBS) at the Uppsala Tandem Laboratory, specifically using 2 MeV ^{4}He ions backscattered at an angle of 170 degrees. The RBS data were fitted to a model of the film–substrate system by use of the SIMNRA program[24]. Film density ρ was ~5.5 g cm^{-3} as computed from

$$\rho = \frac{M \cdot N_s}{n_{atoms} \cdot N_A \cdot d} \quad , \qquad (2)$$

where M is molar mass, N_s is areal density of atoms, n_{atoms} is the number of atoms in a molecule, and N_A is Avogadro's constant.

Electrochemical and optical measurements

Cyclic voltammetry (CV) was performed in a three-electrode electrochemical cell by use of a computer-controlled ECO Chemie Autolab/GPES Interface. The WO_3 film served as working electrode and was electrochemically cycled in 1M $LiClO_4$ dissolved in propylene carbonate. Both counter and reference electrodes were Li foils. CV scans at fixed rate were taken for up to 400 cycles, either at 10 or 20 mV s^{-1}. CV data as a function of scan rate were recorded from high to low scan rate to avoid inadvertent ion trapping during long-term cycling. All electrochemical studies were performed in an argon-filled glove box with water

content below ~0.5 ppm. The electrolyte was prepared by dissolving $LiClO_4$ in propylene carbonate inside the glove box. Both chemicals were fresh and hence considered moisture free. A galvanostatic technique was used to extract Li^+-ions from the WO_3 films; specifically, a constant current was applied in the direction opposite to the one yielding Li^+-ion insertion in the host material. The corresponding potential level (5.5 V or more) will lead to electrolyte degradation[25], which accounts for a large amount of the charge passed. In order to assess this contribution, a control experiment was carried out using a Pt foil as working electrode, as has been recommended in earlier work.[26] Electrolyte degradation may be less important in electrochromic devices using other electrolytes, such as oxide-film-based or polymer-based. Charge capacity was determined from CV data by

$$C = \int \frac{j dV}{s} \quad , \quad (3)$$

where C is charge capacity (mC/cm^2), j is current density (mA/cm^2), s is scan rate (V/s), and V is voltage (in V). The number of inserted and extracted Li^+-ions in Li_xWO_3 was derived from

$$x = \frac{Q \cdot M}{e \cdot A \cdot \rho \cdot d \cdot N_A} \quad , \quad (4)$$

where Q is the inserted charge calculated from CV data, e is elementary charge, and A is intercalated area.

Optical transmittance was measured *in situ* in the 380–800 nm wavelength range during electrochemical cycling of WO_3 films by using a fiber-optical instrument from Ocean Optics. The electrochemical cell was positioned between a tungsten halogen lamp and the detector, and the 100-%-level was taken as the transmittance recorded before immersion of the sample in the electrolyte.

Supplementary Material

Refer to Web version on PubMed Central for supplementary material.

Acknowledgement

We acknowledge support with RBS-measurements from Daniel Primetzhofer and the staff of the Tandem accelerator laboratory at Uppsala University. Assistance was received from Miguel Arvizu and Carlos Triana for sample preparation. The authors would like to thank an anonymous reviewer, whose insightful comments guided us towards a much improved manuscript. Financial support was received from the European Research Council under the European Community's Seventh Framework Program (FP7/2007–2013)/ERC Grant Agreement No. 267234 ("GRINDOOR").

References

1. Llordes A, Garcia G, Gazquez J, Milliron DJ. Tunable near-infrared and visible light transmittance in nanocrystal-in-glass composites. Nature. 2013; 500:323–332. [PubMed: 23955232]
2. Granqvist CG. Electrochromics for smart windows: Oxide-based thin films and devices. Thin Solid Films. 2014; 564:1–38.

3. Niklasson GA, Granqvist CG. Electrochromics for smart windows: Thin films of tungsten oxide and nickel oxide, and devices based on these. J. Mater. Chem. 2007; 17:127–156.
4. Granqvist CG. Electrochromic materials: Out of a niche. Nature Mater. 2006; 5:89–90. [PubMed: 16449991]
5. Granqvist, CG. Handbook of Inorganic Electrochromic Materials. Elsevier; Amsterdam, The Netherlands: 1995.
6. Faughnan BW, Crandall RS, Heyman PM. Electrochromism in WO_3 amorphous films. RCA Rev. 1975; 36:177–197.
7. Hashimoto S, Matsuoka H. Prolonged lifetime of electrochromism of amorphous WO_3–TiO_2 thin films. Surf. Interface Anal. 1992; 19:464–468.
8. Arvizu MA, Triana CA, Stefanov BI, Granqvist CG, Niklasson GA. Electrochromism in sputter-deposited W–Ti oxide films: Durability enhancement due to Ti. Sol. Energy Mater. Sol. Cells. 2014; 125:184–189.
9. Hashimoto S, Matsuoka H. Lifetime and electrochromism of amorphous WO_3–TiO_2 thin films. J. Electrochem. Soc. 1991; 138:2403–2408.
10. Niklasson GA, Malmgren S, Green S, Backholm J. Determination of electronic structure by impedance spectroscopy. J. Non-Cryst. Solids. 2010; 356:705–709.
11. Bressers PMMC, Meulenkamp EA. The electrochromic behavior of indium tin oxide in propylene carbonate solutions. J. Electrochem. Soc. 1998; 145:2225–2230.
12. Li W-J, Fu Z-W. Nanostructured WO_3 thin film as a new anode material for lithium-ion batteries. Appl. Surf. Sci. 2010; 256:2447–2452.
13. Hashimoto S, Matsuoka H, Kagechika H, Susa M, Goto KS. Degradation of electrochromic amorphous WO_3 film in lithium-salt electrolyte. J. Electrochem. Soc. 1990; 137:1300–1304.
14. Bisquert J. Analysis of the kinetics of ion intercalation: Ion trapping approach to solid-state relaxation processes. Electrochim. Acta. 2002; 47:2435–2449.
15. Garcia-Belmonte G, Bueno PR, Fabregat-Santiago F, Bisquert J. Relaxation processes in the coloration of amorphous WO_3 thin films studied by combined impedance and electro-optical measurements. J. Appl. Phys. 2004; 96:853–859.
16. Fabregat-Santiago F, et al. Dynamic processes in the coloration of WO_3 by lithium insertion. J. Electrochem. Soc. 2001; 148:E302–E309.
17. Bisquert J, Vikhrenko VS. Analysis of the kinetics of ion intercalation. Two state model describing the coupling of solid state ion diffusion and ion binding processes. Electrochim. Acta. 2002; 47:3977–3988.
18. Bisquert J. Fractional diffusion in the multiple-trapping regime and revision of the equivalence with the continuous-time random walk. Phys. Rev. Lett. 2003; 91:010602. [PubMed: 12906528]
19. Bisquert J. Beyond the quasistatic approximation: Impedance and capacitance of an exponential distribution of traps. Phys. Rev. B. 2008; 77:235203.
20. Berggren L, Jonsson JC, Niklasson GA. Optical absorption in lithiated tungsten oxide thin films: Experiment and theory. J. Appl. Phys. 2007; 102:083538.
21. Hjelm A, Granqvist CG, Wills JM. Electronic structure and optical properties of WO_3, $LiWO_3$, $NaWO_3$, and HWO_3. Phys. Rev. B. 1996; 54:2436–2445.
22. Yoon S, Woo S-G, Jung K-N, Song H. Conductive surface modification of cauliflower-like WO_3 and its electrochemical properties for lithium-ion batteries. J. Alloys Compounds. 2014; 613:187–192.
23. Knowles TJ. Optical regeneration of aged WO_3 electrochromic cells. Appl. Phys. Lett. 1977; 31:817–818.
24. Mayer M. SIMNRA, a simulation program for the analysis of NRA, RBS and ERDA. Am. Inst. Phys. Conf. Proc. 1999; 475:541–544.
25. Ulfheil J, Würsig A, Schneider OD, Novák P. Acetone as oxidative decomposition product in propylene carbonate containing battery electrolyte. Electrochem. Commun. 2005; 7:1380–1384.
26. Georén P, Lindbergh G. On the use of voltammetric methods to determine electrochemical stability limits for lithium battery electrolytes. J. Power Sources. 2003; 124:213–220.

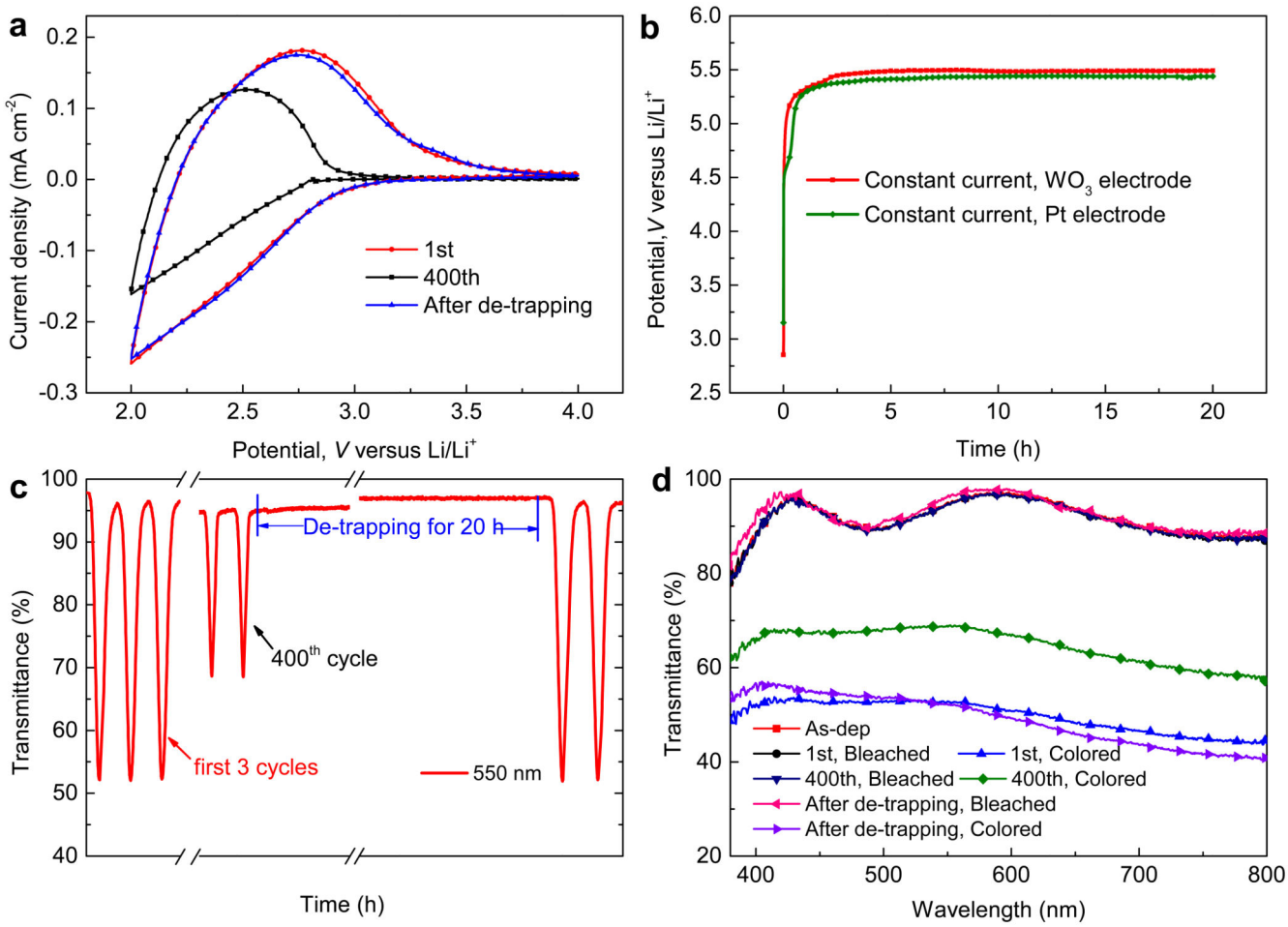

Figure 1. Rejuvenation assessment for WO_3 films

(**a**) CV data at different cycle numbers for a scan rate of 20 mV s^{-1}. (**b**) Voltage upon extraction of trapped ions for WO_3 film and Pt electrodes. The constant current was 1×10^{-5} A cm^{-2}. (**c**) and (**d**) Optical transmittance at 550 nm and in the visible spectral range, respectively, at different cycle numbers. Spectral transmittance data overlap for the bleached state, except after ion de-trapping where the data differ marginally.

Europe PMC Funders Author Manuscripts

Europe PMC Funders Author Manuscripts

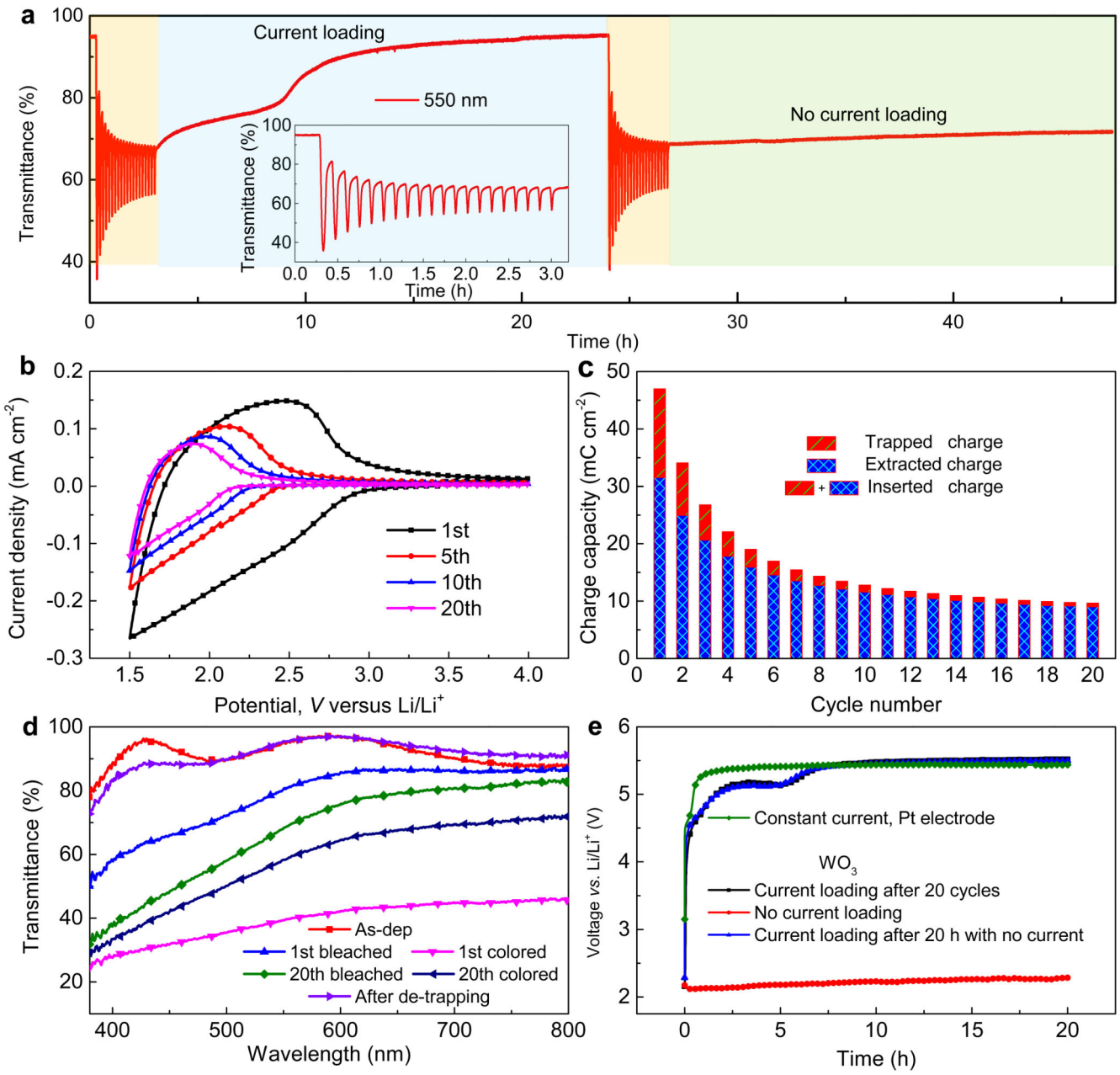

Figure 2. Electrochromic performance of WO_3 films under varied operations

(**a**) Comparison of optical response at 550 nm and for 1.5–4.0 V with and without constant loading current; inset shows a magnified view of the transmittance during 20 initial cycles at 10 mV s^{-1}. (**b**) CV data for different cycle numbers at 10 mV s^{-1}. (**c**) Trapped and extracted charge densities *vs.* cycle number derived from CV data. (**d**) Optical transmittance for the film in as-deposited state, after bleaching and coloring for the indicated number of cycles, and after galvanostatic ion extraction. (**e**) Voltage *vs.* time for WO_3 films with and without constant current. The electrolyte response obtained with a Pt electrode is shown for comparison.

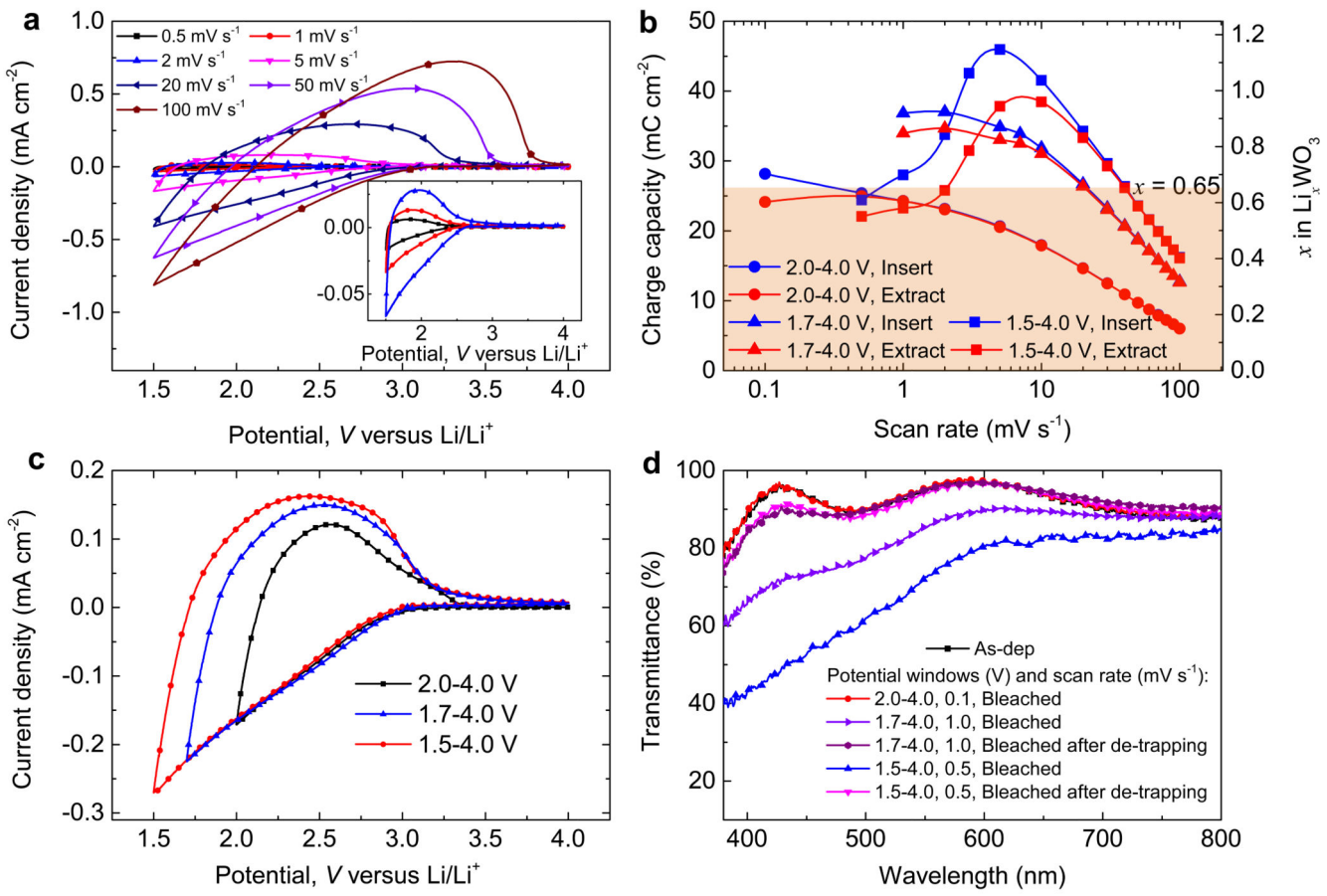

Figure 3. Dynamics of ion trapping and de-trapping in WO_3 thin films

(**a**) Cyclic voltammograms of films at various scan rates recorded for 1.5–4.0 V; inset shows vertically magnified data for the lowest scan rates. (**b**) Charge capacity *vs.* scan rate for films with charge extracted/inserted in the shown potential windows; right-hand axis indicates the amount of Li^+-ions as x in Li_xWO_3. (**c**) CV data for different potential windows recorded at 10 mV s^{-1}. (**d**) Optical transmittance of films in as-deposited state and subjected to various procedures for ion-trapping (different potential windows, scan rates, and galvanostratic ion de-trapping). Spectral data for the as-deposited state and after bleaching at 2.0–4.0 V are overlapping, as are data for the bleached state of de-trapped films.

Europe PMC Funders Author Manuscripts

Europe PMC Funders Author Manuscripts

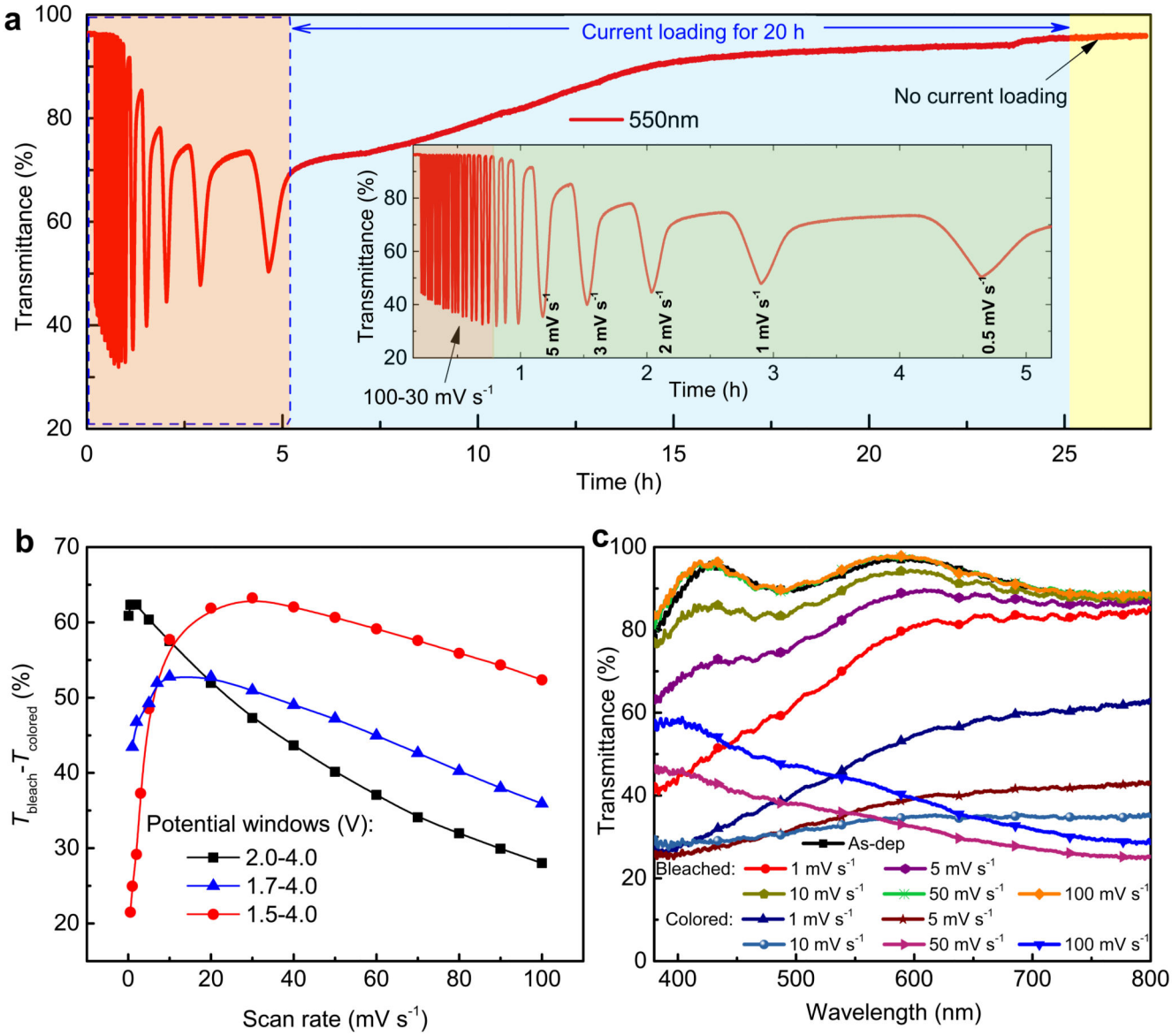

Figure 4. Ion-trapping-induced optical performance of WO_3 thin films

(**a**) *In situ* optical transmittance at 550 nm and at varying scan rates recorded at 1.5–4.0 V; inset is a close-up for short times. (**b**) Optical modulation ($T_{bleach} - T_{colored}$) at 550 nm for different scan rates at 1.5–4.0 V for different potential windows. (**c**) Spectral transmittance at different scan rates for an as-deposited film and for this film in bleached and colored state.